Zhu et al. Respiratory Research (2024) 25:291
https://doi.org/10.1186/s12931-024-02926-8

Respiratory Research

RESEARCH Open Access

Glycolytic enzyme PGK1 promotes M1 macrophage polarization and induces pyroptosis of acute lung injury via regulation of NLRP3

Guiyin Zhu[1†], Haiyang Yu[1†], Tian Peng[1], Kun Yang[1], Xue Xu[1] and Wen Gu[1*]

Abstract

Acute lung injury (ALI) is characterized by an unregulated inflammatory reaction, often leading to severe morbidity and ultimately death. Excessive inflammation caused by M1 macrophage polarization and pyroptosis has been revealed to have a critical role in ALI. Recent study suggests that glycolytic reprogramming is important in the regulation of macrophage polarization and pyroptosis. However, the particular processes underlying ALI have yet to be identified. In this study, we established a Lipopolysaccharide(LPS)-induced ALI model and demonstrated that blocking glycolysis by using 2-Deoxy-D-glucose(2-DG) significantly downregulated the expression of M1 macrophage markers and pyroptosis-related genes, which was consistent with the in vitro results. Furthermore, our research has revealed that Phosphoglycerate Kinase 1(PGK1), an essential enzyme in the glycolysis pathway, interacts with NOD-, LRR- and pyrin domain-containing protein 3(NLRP3). We discovered that LPS stimulation improves the combination of PGK1 and NLRP3 both in vivo and in vitro. Interestingly, the absence of PGK1 reduces the phosphorylation level of NLRP3. Based on in vitro studies with mice bone marrow-derived macrophages (BMDMs), we further confirmed that siPGK1 plays a protective role by inhibiting macrophage pyroptosis and M1 macrophage polarization. The PGK1 inhibitor NG52 suppresses the occurrence of excessive inflammation in ALI. In general, it is plausible to consider a therapeutic strategy that focuses on modulating the relationship between PGK1 and NLRP3 as a means to mitigate the activation of inflammatory macrophages in ALI.

Keywords Macrophage polarization, Pyroptosis, Glycolytic reprogramming, Acute lung injury

†Guiyin Zhu and Haiyang Yu contributed equally to this work.

*Correspondence:
Wen Gu
guwen@xinhuamed.com.cn
[1]1Department of Respiratory Medicine, Xinhua hospital, Shanghai Jiao Tong University School of Medicine, 1665 KongJiang road, shanghai 200092, China

Introduction

Acute lung injury (ALI) is a progressive respiratory syndrome with significant morbidity and mortality in the world [1]. Currently, symptomatic and supportive treatment of ALI is still emphasized [2]. Therefore, it is of great importance for us to find effective ways to attenuate the pulmonary overwhelming inflammation in ALI. It is well known that alveolar macrophages play a pivotal role in the recognition and clearance of pathogens [3]. Activated macrophages would intensify the pulmonary inflammation cascade by releasing pro-inflammatory cytokines [4]. Though the over-activation of macrophages plays a crucial role in the onset and progression of ALI, mechanisms responsible for macrophages activation in ALI remains largely unknown.

Under diverse micro-environments, macrophages exhibit two major categories: LPS-induced pro-inflammatory M1 and IL4/IL13-induced anti-inflammatory M2 macrophages. Macrophages are mainly polarized toward the M1 phenotype in the progression of ALI [5]. In addition, accumulating evidences also suggested that pyroptosis of macrophages may contribute to excessive inflammation in ALI. Pyroptosis is a proinflammatory cell death type characterized by pore formation in the plasma membrane, which is initiated by inflammasomes [6]. The NLRP3 inflammasome is currently the most well-characterized inflammasome and leads to maturation of the proinflammatory cytokines such as IL-1β and IL-18 [7]. Furthermore, recent studies have demonstrated that pyroptosis is associated with macrophage polarization [8].

Of interest, mounting evidences suggested that cellular metabolic alteration that occur in immune cells has a great impact on their function. Elevated aerobic glycolysis was found in proinflammatory macrophages [9]. It has been found that enhanced glycolysis in ALI can influence macrophage polarization and NLRP3 inflammasome activation [10, 11]. Blocking glycolysis could partially ameliorate the hyperactivation of inflammation in LPS-induced ALI [12]. Therefore, a more specific understanding of mechanisms underlying glycolytic reprogramming in macrophage polarization and pyroptosis is urgent and may provide a novel therapeutic target for inflammatory cascade in ALI.

Among the several genes associated with glycolysis, Phosphoglycerate kinase 1 (PGK1) stands out due to its potential for dual functionality. PGK1 is the first ATP-producing enzyme in the glycolytic pathway through transforming 1,3-bisphosphoglycerate (1,3-BPG) to 3-phosphoglycerate (3-PG) [13, 14].Consistent with its overexpression in various human cancer, PGK1 is a critical regulatory factor of tumor progression [15]. Aside from its function as metabolic enzyme, recent studies have elucidated that PGK1 is involved in many biological processes as a kinase. Moreover, loads of works have been reported that PGK1 inhibitor exerts a powerful anti-inflammatory effect [16]. Nevertheless, the precise role of PGK1 in inducing inflammation in ALI is still poorly understood.

Hence, the current study was designed with the objective of examining the following research questions:1) Does glycolytic reprogramming regulate macrophage polarization and pyroptosis in ALI? 2) Can glycolytic enzyme PGK1 regulate the excessive inflammation caused by M1 macrophage activation and pyroptosis in ALI? 3) What are the fundamental mechanisms that underlie the relationship between PGK1 and NLRP3 in ALI?

Methods and materials

Experimental animals and acute lung injury model

Wild-type (WT) male C57BL/6J mice, aged 6–8 weeks, were sourced from Shanghai Slack Experiment Co., Ltd. These mice were accommodated in a controlled, pathogen-free environment at the Xinhua Hospital Animal Laboratory in Shanghai, China. All animal experiments were conducted in accordance with the approved protocols by the Ethics Committee of Xinhua Hospital, affiliated with the Shanghai Jiao Tong University School of Medicine (Approval No, XHEC-F-2023-067). The acute lung injury (ALI) model was induced through intranasal administration of LPS (from E. coli O111:B4, Sigma-Aldrich, MO, USA) at a dose of 5 mg/kg for 24 h. The control group received an equivalent volume of the solvent. The glycolysis inhibitor 2-deoxy-D-glucose (2-DG) (1 g/kg, HY-13966, MCE, USA) was administered via intraperitoneal injection 1 h prior to the LPS treatment as previously described [12]. Mice were administered NG52(HY-15154, MCE, USA) intragastrically at dosages of 50, 100, or 150 mg/kg 1 h before the LPS treatment [17, 18]. At the end of the experiment, the mice were euthanized and subjected to a series of analyses as outlined below.

Lung histological analysis and inflammatory injury score

The right upper lung lobes of the mice were fixed in 4% paraformaldehyde overnight, subsequently embedded in paraffin, sectioned, and stained with hematoxylin-eosin. A predefined scoring system was employed to semi-quantify the degree of histological lung injury [19]. The system encompassed four parameters: alveolar septal thickening, inflammation, hemorrhage, and edema, with severity scores varying from 0 to 4.

BMDM Culture and Treatment

6-week-old mice were humanely euthanized. Bone marrow was then extracted from the tibia and fibula. The cells were cultured in Dulbecco's minimum essential

medium(DMEM) containing 20% L929 supernatant and 10% fetal bovine serum (FBS) and 1% penicillin/streptomycin(P/S). On the 7th day. BMDMs were treated with LPS (100ng/ml) for M1 polarization model. And the cells were pre-stimulated with LPS (500ng/ml) for a duration of 4 h. This was followed by stimulation with ATP (5mM, MCE, USA) for pyroptosis model. In order to assess the impact of glycolysis on macrophages, we administered 2-DG (5mM, HY-13966, MCE, USA) to the cells prior to stimulating them. The small interfering RNA (siRNA) was manufactured by Gene Pharma (Shanghai, China). The sense sequence of siPGK1 is 5′-GCGCUAAAGUUGCAGACAATT-3′. The transfection of siPGK1 was carried out using Rfect siRNA/miRNA Transfection Reagent (Baidai biotechnology, Changzhou, China) according to the manufacturer's recommendations. The silencing efficacy of the target genes was confirmed using Western blot analysis.

Western blotting (WB)

Lung tissues and cells were harvested and lysed using RIPA lysis buffer. Subsequently, centrifugation was carried out, and the samples were denatured using loading buffer. The proteins were separated by 10-12.5% SDS-PAGE and transferred to PVDF membranes. The membranes were incubated with corresponding primary antibodies at 4℃ overnight. The following primary antibodies were used: anti-NLRP3(CST, D4D8T), anti-GSDMD(abcam, ab209845), anti-IL-1β(santa cruz, sc-12742), anti-HK2(santa cruz, sc-130358), anti-LDHA (Proteintech, 19987-1-AP), anti-PKM2(abclonal, A20991), anti-iNOS(CST, 13120), anti-PGK1(Proteintech, 17811-1-AP; santa cruz, sc-130335), anti-α-Tubulin(Proteintech, 11224-1-AP). On the following day, the membranes were incubated with secondary antibodies (Beyotime, China) at room temperature for 1 h. The protein bands were visualized using an enhanced chemiluminescence reagent, and the relative protein expression was quantified using the Image J system.

Real-time quantitative PCR

Total RNA was extracted using TRIzol (TAKARA, Japan) according to the manufacturer's instructions. Prime Script RT Master Mix (TAKARA, Japan) was utilized for cDNA synthesis, and subsequently amplified with Hieff qPCR SYBR Green Master Mix (Low Rox Plus) (YEASEN, China) on the QuantStudio™ 3 System (Applied Biosystems). Relative expression levels were calculated using the 2^-ΔΔCt method. Primer sequences are provided in Table 1.*Sequences of the primers*.

Table 1 Sequences of the primers

	Forward primer (5′-3′)	Reverse primer (5′-3′)
Hk2	GCGTGGATGGCTCTGTCTAC AAG	GGAGGAAGCGGACATCAC AATCG
Pkm2	GCCGCCTGGACATTGACTC	CCATGAGAGAAATTCAGC CGAG
Ldha	TGTCTCCAGCAAAGACTACTGT	GACTGTACTTGACAATGTT GGGA
Actb	AGAGGGAAATCGTGCGTGAC	CAATAGTGATGACCTGGCCGT

Flow cytometry analysis

A total of 1×10^6 cells were harvested through centrifugation and subsequently resuspended in PBS for the purpose of flow cytometry analysis. Anti-CD86 (BioLegend, USA), and anti-F4/80 (BioLegend, USA) antibodies were employed for fluorescent staining following the manufacturer's instructions. The cell suspensions, following the incubation period, were subjected to analysis using the CytoFLEX flow cytometer (Beckman, USA). The results were analyzed using FlowJo v10 software (Tree Star Inc.).

Immunofluorescence and immunohistochemistry

For immunofluorescence analysis, BMDMs were cultured on glass coverslips placed in 12-well plates. The cells were immobilized using a 4% paraformaldehyde (Solarbio, Beijing, China) for 10 min. Subsequently, Immunostaining Permeabilization Solution with Triton X-100(Beyotime, China) was applied to permeabilize the cells for 10 min. To prevent non-specific binding, the cells were blocked with Immunol Staining Blocking Buffer (Beyotime, China) at room temperature for 15 min. The cells were treated with primary antibodies overnight at a temperature of 4℃. The following primary antibodies were used: iNOS (CST, 13120), PGK1(proteintech,17811-1-AP), NLRP3(Proteintech,19771-1-AP), Caspase 1/p20/p10 (Proteintech, 22915-1-AP). Subsequently, the cells were incubated with secondary antibodies coupled with FITC/Cy3 at room temperature for a duration of 1 h. Following this, the cells were subjected to staining with DAPI for 5 min.

The sections underwent a dewaxing and rehydration process using xylene and various concentrations of alcohol. Then the paraffin sections underwent incubation with a 3% hydrogen peroxide solution. Subsequently, antigen retrieval was performed by subjecting the sections to microwave heating. Finally, the specimens were treatment with goat serum in order to inhibit nonspecific reactions. The sections were labelled with the primary antibody targeting iNOS (Servicebio, China). Subsequently, the sections were treated with secondary antibodies at a temperature of 37 °C for a duration of 1 h. After that, the sections were subjected to diaminobenzidine (DAB) staining, and then the nuclei were stained with hematoxylin. The samples that were made were then seen using an optical microscope.

Lactate assay

Lactate concentrations in the media were determined using a lactic acid test kit (Nanjing Jiancheng Bioengineering Institute, Nanjing, China). The lung tissue of the mice was mixed with physiological saline solution at a weight ratio of 1:9. The combination underwent mechanical homogenization while being kept in an ice bath. Following a centrifugation process lasting 10 min at a speed of 2,500 rpm, the supernatant was gathered for further examination. The absorbance of the samples was measured at a wavelength of 530 nm. The protein concentrations were employed for the purpose of standardizing these values.

Transmission electron microscope(TEM)

The lung tissue of the mice was implanted in epoxy glue and later cut into sections. The specimens, which had dimensions ranging from 60 to 80 nm, underwent staining with a 2% solution of uranium acetate. The investigation of cell membrane perforation was conducted with the TECNAI G2 20 TWIN transmission electron microscope (TEM).

Immunoprecipitation followed by mass spectrometry (IP-MS) and co-immunoprecipitation (co-IP)

The Protein A/G beads (Beyotime, China) were mixed with anti-NLRP3 antibody(CST, D4D8T) for 1 h at room temperature. The cells were subjected to extraction using an IP lysis buffer (Beyotime, China). The whole-cell lysates were mixed with beads-antibody complex overnight at 4 °C. The utilisation of anti-IgG was employed as a negative control in the experiment. Following washing, the complex was eluted and submitted to denaturation. The samples were loaded onto a polyacrylamide gel. Subsequently, the gel was stained with coomassie brilliant blue. The proteins were analyzed utilizing Thermo Fisher LTQ Obitrap ETD(Thermo, USA).

The Co-Immunoprecipitation (Co-IP) test was employed to ascertain the interacting protein. Initially, the IP procedure, as previously delineated, was executed. Subsequently, the immunoprecipitates utilizing anti-NLRP3 (CST, D4D8T), anti-PGK1 (santa cruz, sc-130335) and Anti-Phosphoserine/threonine (ECM Biosciences, PP2551) antibodies were employed for Western blot validation.

Molecular docking

The three-dimensional structure models of proteins PGK1(P00558) and NLRP3(Q96P20) were downloaded from the Uniprot database. The ATP/ADP binding site on PGK1 was found using Autodock1.5.7 by docking ATP/ADP with it in order to locate the kinase domain of PGK1. The HDOCK tool (http://hdock.phys.hust.edu.cn/) is used to compute protein-protein docking. The PYMOL software is utilized for the three-dimensional visualization of complexes.

Enzyme linked immunosorbent assay (ELISA)

The bronchoalveolar lavage fluid(BALF) levels of IL-1β in the mice were quantified using an ELISA kit (Aifang Biotechnology Co., Ltd, Hunan, China).The measurements were conducted following the instructions provided by the manufacturer.

Statistical analysis

The experiment in this study was conducted with a minimum of three repetitions and the data were presented in the form of mean ± standard error of the mean (SEM). An unpaired two-tailed Student's t-test was employed to compare the means of two groups. In the case of three groups, the statistical analysis employed was one-way analysis of variance (ANOVA). A p-value less than 0.05 was considered to be statistically significant. The statistical analyses were performed using GraphPad Prism 9.5.1 (San Diego, CA, USA).

Results

M1 macrophage activation and pyroptosis in ALI mice

For the beginning of the result part, we established a LPS-induced ALI model by nasal drip to explore the inflammatory response of macrophages in vivo. HE staining results showed that there was significant inflammation infiltration in the lung tissue of the ALI group compared with the CON group (Fig. 1A-B). What's more, Immunohistochemistry results indicated that the expression marker iNOS was significantly upregulated in the lung tissue of the ALI group (Fig. 1C). Therefore, there is an infiltration of M1 mcarophages in the lung tissue of ALI mice. Western blotting further confirmed high expression of pyroptosis-related proteins NLRP3, GSDMD and IL1β in ALI mice (Fig. 1D-E). Morphologically, the results of transmission electron microscopy (TEM) showed that macrophages in lung tissue of ALI group had cell membrane perforation(Fig. 1F). Briefly, these data suggest that macrophages are polarization to M1 phenotype and occur pyroptosis in ALI mice.

Blocking glycolysis alleviates lung injury in ALI mice by reducing M1 macrophage polarization and pyroptosis

Next, we aimed to elucidate whether glycolysis was upregulated in ALI. Compared with the CON group, WB results showed that the expression of glycolysis-related enzymes HK2, PKM2 and LDHA at the protein level were significantly up-regulated (Fig. 2A-B). The same trend was also demonstrated in q-PCR results, except Ldha (Fig. 2C).Next, we firstly determined 2-DG(a glycolysis inhibitor) to further verify the relationship between enhanced glycolysis and inflammation in ALI.

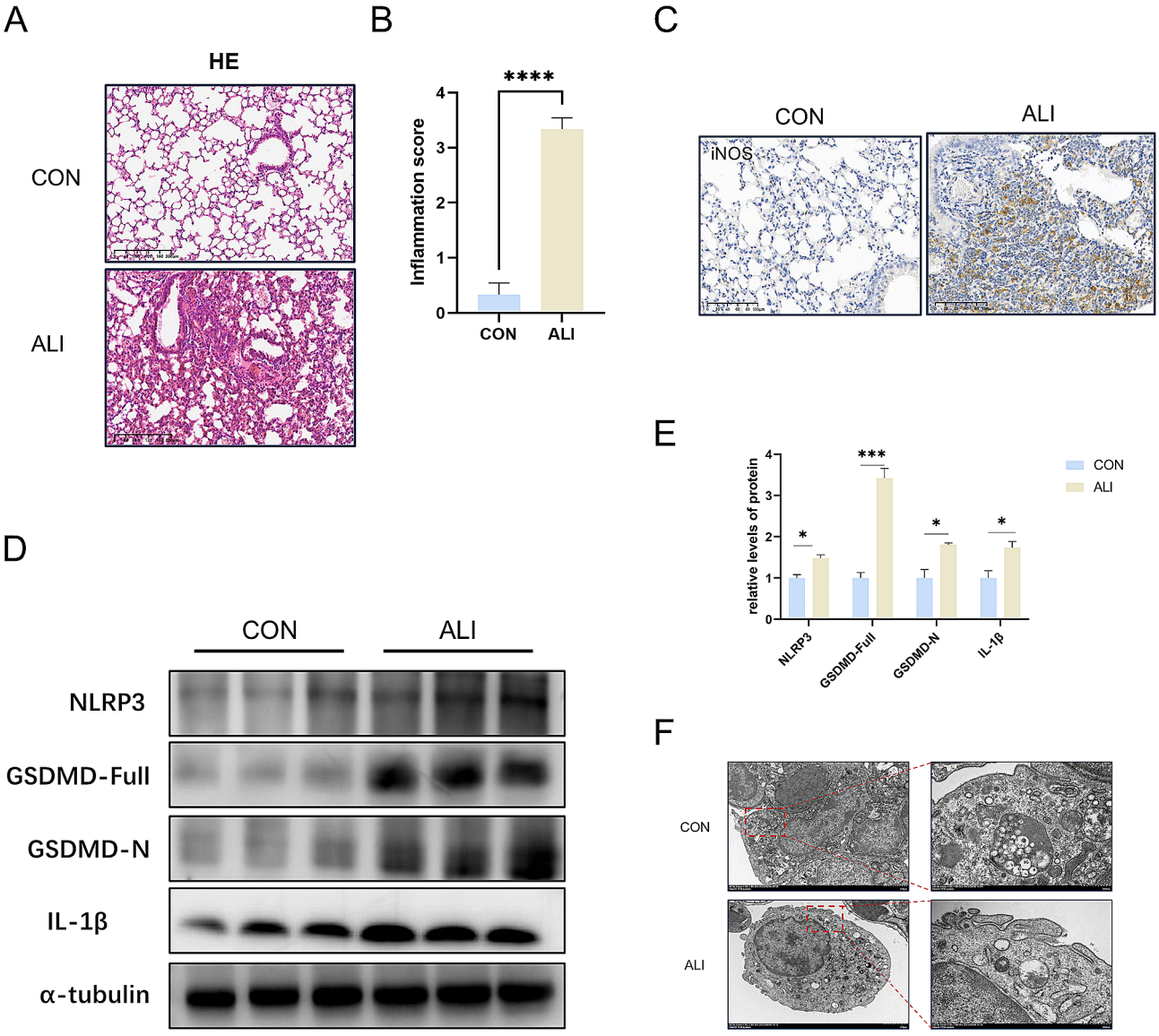

Fig. 1 M1 macrophage activation and pyroptosis in ALI mice. **A**-**B**: C57BL/6J mice were administered with Lipopolysaccharide(LPS) for 24 h as a model of acute lung injury(ALI). Representative images (scale bar 200 μm) of histological lung sections stained with hematoxylin-eosin from CON and ALI group mice. **C**: immunohistochemical (IHC) staining analyses the expression of M1 macrophages associated molecular iNOS in lung tissues(scale bar 100 μm). **D**-**E**: Western blotting analyses the expression of pyroptosis molecules NLRP3, GSDMD, IL-1β in lung. Immunoblot analysis of pyroptosis molecules NLRP3, GSDMD, IL-1β expression in lung, compared with the CON group. **F**: Electron microscopy analyses membrane perforations of macrophages in lung tissue (scale bar 2.0 μm; scale bar 500 nm). The data shown are the means ± SEM obtained from three separate biological replicates. * $P < 0.05$, *** $P < 0.001$, **** $P < 0.0001$ by unpaired t test

The 2-DG intervention attenuated histological lesions in the lung compared with ALI group (Fig. 2D-E). We also found that relative lactate content was significantly decreased after 2-DG treatment (Fig. 2F). Indeed, the production of IL-1β in the BALF that was induced by LPS was reduced by 2-DG(Fig. 2G). What' more, Western blotting showed that 2-DG decreased the expression of pyroptosis-related genes such as NLRP3, GSDMD and IL-1β(Fig. 2H-I) compared to ALI mice. Meanwhile, TEM results showed that the degree of cell membrane perforation of macrophages in lung tissue was reduced after 2-DG intervention (Fig. 2J). Furthermore, we found that 2-DG significantly downregulated the M1 macrophage ($iNOS^+$ cells) as assessed by immunohistochemistry (Fig. 2K). These observations indicate that blockage of glycolysis by 2-DG weaken M1 macrophage polarization and pyroptosis.

Blocking glycolysis inhibits macrophage polarization to M1 phenotype and alleviates pyroptosis in vitro

Given the possible regulatory role of glycolytic reprogramming in inflammation, we next asked whether

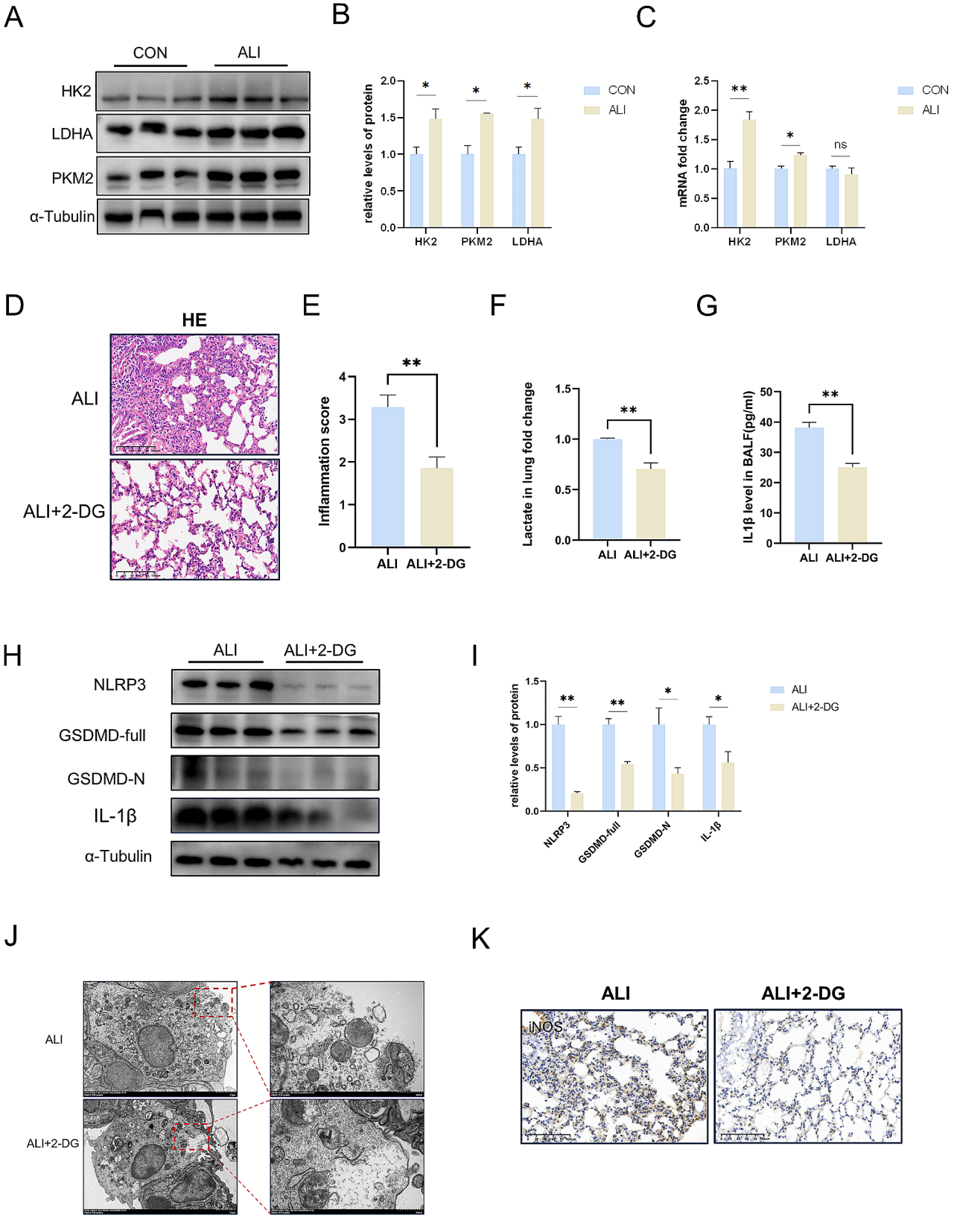

Fig. 2 (See legend on next page.)

(See figure on previous page.)

Fig. 2 Blocking glycolysis alleviates lung injury in ALI mice by reducing M1 macrophage polarization and pyroptosis **A**-**B**: The expression levels of HK2, PKM2, LDHA in lung tissues were measured by Western blot. Immunoblot analysis of glycolytic protein HK2, PKM2, LDHA expression in lung, compared with the CON group. **C**: Detection of glycolysis-related genes Hk2, Pkm2, Ldha mRNA expression in the lung tissues by RT-qPCR. **D**-**E**: C57BL/6J mice were intraperitoneally injected with 2-DG 1 h before the LPS administration. Evaluation of the therapeutic effect of 2-DG on the lung tissue of ALI mice by HE staining (scale bar 100 μm). Inflammation score was measured. **F**: Lactate concentration in lung lysate was assayed. **G**:The ELISA assay was employed to quantify the concentration of IL-1β in the bronchoalveolar lavage fluid (BALF). **H**-**I**: Protein levels of NLRP3, GSDMD, IL-1β in lung were determined by Western blotting. **J**: Electron microscopy analyses membrane perforations of macrophages in lung tissue(scale bar 2.0 μm; scale bar 500 nm). **K**: IHC for iNOS in the lung tissue (scale bar 100 μm). The data shown are the means ± SEM obtained from three separate biological replicates. * $P < 0.05$, ** $P < 0.01$ by unpaired t test

enhanced glycolysis was required for macrophage M1 polarization and pyroptosis in BMDMs. It was found that the treatment of 2-DG reversed the upregulation of M1 marophage marker CD86 assessed by flow cytometry (Fig. 3A). Interestingly, compare to LPS group, macrophages also exhibited a lower level of M1 marker iNOS after being treated with 2-DG in vitro (Fig. 3B-D). Compare to LPS+ATP group, double immunofluorescence staining indicated that 2-DG decreased the expression of NLRP3 and Caspase1 (Fig. 3E). These data suggest that inhibition of glycolysis by 2-DG downregulated inflammatory response in BMDMs.

An interaction exists between PGK1 and NLRP3 in BMDMs under the stimulation of LPS

Next, we sought to understand the mechanism through which enhanced glycolysis effected NLRP3 inflammasome activation. Based on the critical role of NLRP3 inflammasome played in M1 macrophage and macrophage pyroptosis [20, 21].Therefore, we treated BMDMs with LPS of which total cell lysates was incubated with a specific anti-NLRP3 antibody. Using the mass spectrometry, the results demonstrated that 473 candidate proteins binding with NLRP3. Next, we projected the mouse genes onto human genes with R package "biomaRt". We then intersected the differentially expressed gene list from aerobic glycolysis related gene list from the msigdb database (Fig. 4A). There were 4 genes (ENO1, ALODA, SLC2A1, PGK1). Among them, PGK1 which are the only two ATP-generating enzymes in the glycolysis pathway attracted our attention. Emerging evidence showed that PGK1 is not only a metabolic enzyme, but also function as protein kinase which could phosphorylate various protein substrates to regulate intracellular signal transduction pathways [22]. In addition, we found that the expression of PGK1 was highest in macrophages in lung tissue through The Human Protein Atlas (HPA) database (Fig. 4B). It partially illustrated the feasibility of studying PGK1 in regulating the function of macrophages. Next, the interaction between PGK1 and NLRP3 was investigated under physiological conditions by immunoprecipitation (IP). An association between PGK1 and NLRP3 was detected in LPS-stimulated BMDMs (Fig. 4C). Moreover, immunofluorescence analysis demonstrated a pronounced colocalization of PGK1 and NLRP3 within the LPS-treated group (Fig. 4D). Western blotting results revealed a consistent upregulation of both PGK1 and NLRP3 expression at multiple time points, specifically at 6 h, 12 h, and 24 h post-LPS treatment, in comparison to the 0 h group (Fig. 4E-G). The significant increase in PGK1 expression in response to LPS strongly suggests its potential involvement in the activation of the NLRP3 inflammasome pathway. On the whole, these results indicate that PGK1 could interact with NLRP3.Futhermore, PGK1 exhibited an elevated expression under LPS stimulation consistent with NLRP3.

The association between PGK1 and NLRP3 exhibited an increased affinity after being stimulated by LPS

The aforementioned findings provide confirmation of an observed interaction between variables PGK1 and NLRP3 within the LPS-treated in vitro group. Subsequently, we sought to ascertain whether there was any alteration in their binding within the LPS-treated group in comparison to the CON group. The results obtained from Co-IP experiments demonstrated that the interaction between PGK1 and NLRP3 exhibited an increased affinity following stimulation with LPS (Fig. 5A-B). Furthermore, using in vivo investigations, we observed an augmented association between the two variables in a mouse model of ALI (Fig. 5C-D). Further, we aimed to investigate the specific structural regions inside the protein that facilitate the formation of this protein interaction. Given PGK1's function as a protein kinase and the stimulating effect of phosphorylation modification on NLRP3, we propose that PGK1 functions as a protein kinase to regulate NLRP3 by phosphorylation modification during the development of ALI. Thereby, we downloaded the three-dimensional structure models of proteins PGK1(P00558) and NLRP3(Q96P20) from the Uniprot database. Using Autodock, we aim to identify the ATP/ADP binding site on PGK1 by docking ATP/ADP with it, in order to locate the kinase domain of PGK1. The HDOCK tool(http://hdock.phys.hust.edu.cn/)is utilized for the computation of protein-protein docking. In this instance, a model has been selected wherein the NLRP3 and the PGK1 are linked with a binding affinity score of -230.08, and the confidence score is 0.8322. PYMOL software is used for 3D visualization of complexes (Fig. 5E-F). Our analysis revealed that the amino acids N31 and K75 in PGK1 and

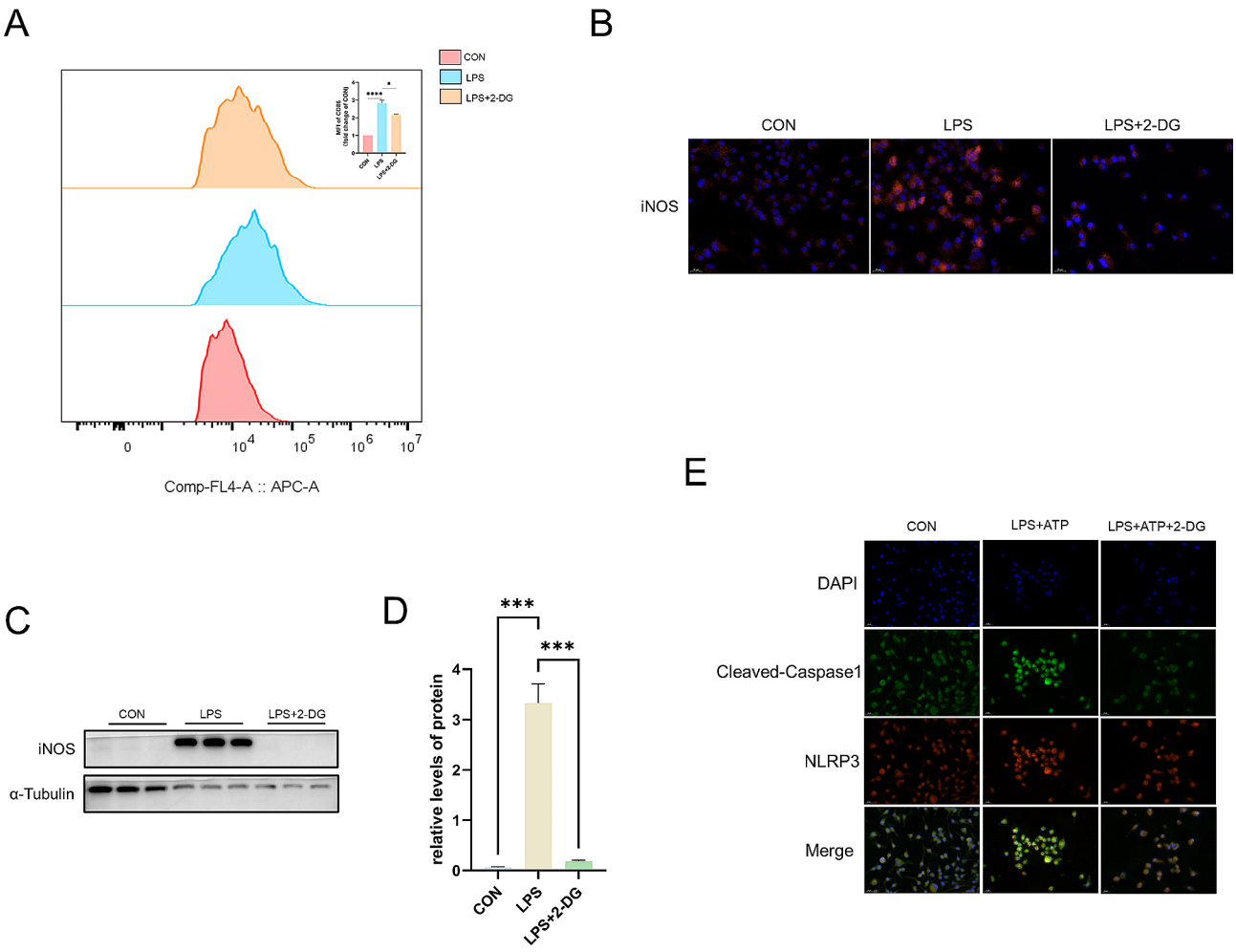

Fig. 3 Blocking glycolysis inhibits macrophage polarization to M1 phenotype and alleviates pyroptosis in vitro **A**-**D**: Bone marrow-derived macrophages (BMDMs) were treated with LPS for 24 h to mimic M1 macrophages. The cells were pre-treated with 2-DG before being stimulated. Flow cytometry detection of CD86 expression on BMDMs after being gated with macrophage marker F4/80. MFI analysis of CD86 expression in BMDMs (**A**). Immunohistofluorescence staining for iNOS(red) (scale bar 20 μm) (**B**). Protein levels of M1 macrophage marker iNOS in BMDMs were determined by Western blotting (**C**-**D**). **E**: The cells were pre-stimulated with LPS for a period of 4 h. Subsequently, the cells were stimulated with ATP to induce the pyroptosis model. Prior to being stimulated, the cells received a 2-DG pretreatment. Immunofluorescence staining for the colocalization of NLRP3(Red) and Cleaved-caspase1(Green) (scale bar 20 μm). The data shown are the means ± SEM obtained from three separate biological replicates. * $P < 0.05$, *** $P < 0.001$, **** $P < 0.0001$ by one-way ANOVA

909 S and 910T in NLRP3 establish two robust hydrogen bonds, respectively. The phosphate moiety of ADP is in close proximity to the residues S852, T853, and S854 of NLRP3. If ATP/ADP tracks the motion of PGK1, there is a strong probability that a phosphorylation modification process will take place at the S852, T853, and S854 residues of NLRP3.The protein-protein docking results have yielded a structural foundation for the possible enzymatic function of PGK1 in its interaction with NLRP3.In brief, our research revealed that PGK1 has the potential to act as a protein kinase, thereby regulating NLRP3 through phosphorylation modification in the course of ALI, whereby the combination of the two is further strengthened in the context of intervention.

Inhibition of PGK1 mitigates M1 macrophages and reduces pyroptosis

To explore the hypothesis mentioned above, BMDMs were transfected with PGK1 short interfering RNA. The efficacy of PGK1 siRNA in suppressing the target gene was affirmed through Western blot analysis (Fig. 6A-B). In order to identify the potential regulatory mechanisms of PGK1 on NLRP3 in BMDMs, we assessed the phosphorylation level of NLRP3 via Co-IP following PGK1 knockdown. The results demonstrated that suppressing PGK1 decreased the degree of phosphorylation of NLRP3 upon LPS stimulation (Fig. 6C). Silencing PGK1 with siRNA resulted in the reduction of the M1 macrophage marker CD86 in F4/80-positive cells following LPS treatment (Fig. 6D). Furthermore, the immunofluorescence

A

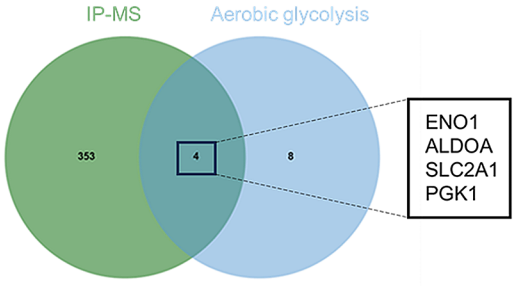

NLRP3 complex(LPS)

Gene names	MW[kDa]	Protein score	Sequence coverage(%)	Unique Peptides	Peptides	PSMs
Nlrp3	118.20	0.83	0.97	1	1	1
Pgk1	44.52	6.16	11.99	3	3	3

B

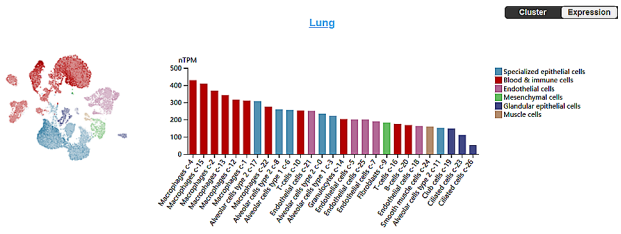

C

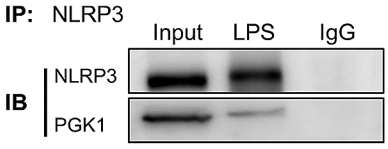

D

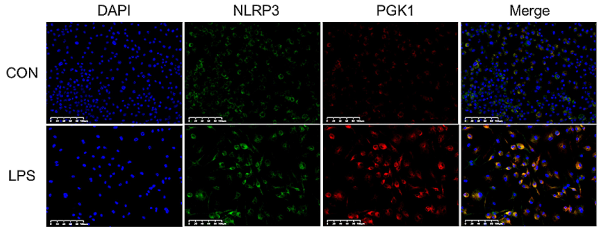

E

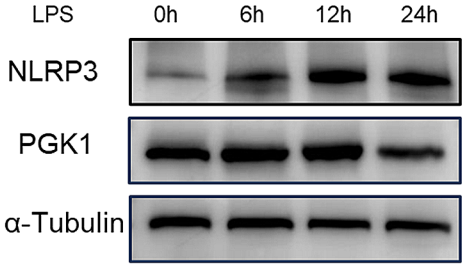

F

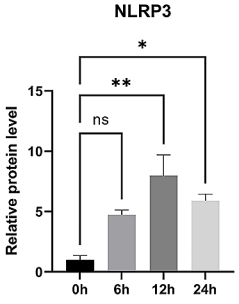

G

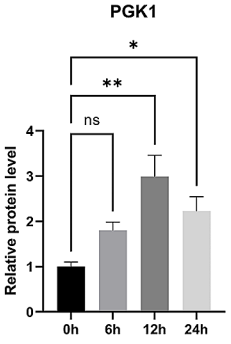

Fig. 4 An interaction exists between PGK1 and NLRP3 in BMDMs under the stimulation of LPS **A**: BMDMs were exposed to LPS for a duration of 24 h in order to model the features of inflammatory macrophages. The intersection analysis of the correlation between NLRP3 IP-MS and the aerobic glycolysis gene set (M39816) from the msigdb database. Identification of PGK1 as a potential NLRP3 interactor in LPS-stimulated BMDMs by mass spectrum primed with LPS. **B**: PGK1 expression in different cells of lung tissue from The Human Protein Atlas (HPA) database. **C**:Co-IP analysis of endogenous association between PGK1 and NLRP3 in LPS-stimulated BMDMs. **D**: Immunofluorescence staining for the colocalization of NLRP3(Green) and Cleaved-caspase1(Red) (scale bar 100 μm). **E**-**G**: Western blotting of NLRP3 and PGK1 protein levels at different times. The data shown are the means ± SEM obtained from three separate biological replicates. * $P < 0.05$, ** $P < 0.01$, ns, not significant by one-way ANOVA

results indicate a reduction in iNOS expression under LPS stimulation after interfering PGK1(Fig. 6E). The above results indicate that inhibiting PGK1 diminishes M1 polarization. In the study of how PGK1 influences macrophage pyroptosis, we established an in-vitro pyroptosis model by stimulating macrophages with LPS and ATP. Compared to the si-CON group, the down-regulation of PGK1 led to a reduction in the expression of GSDMD (Fig. 6F-H). The immunofluorescence analysis demonstrated a reduced colocalization of PGK1 and NLRP3 in the si-PGK group (Fig. 6I). Briefly, the inhibition of PGK1 could attenuate macrophage M1 polarization and pyroptosis.

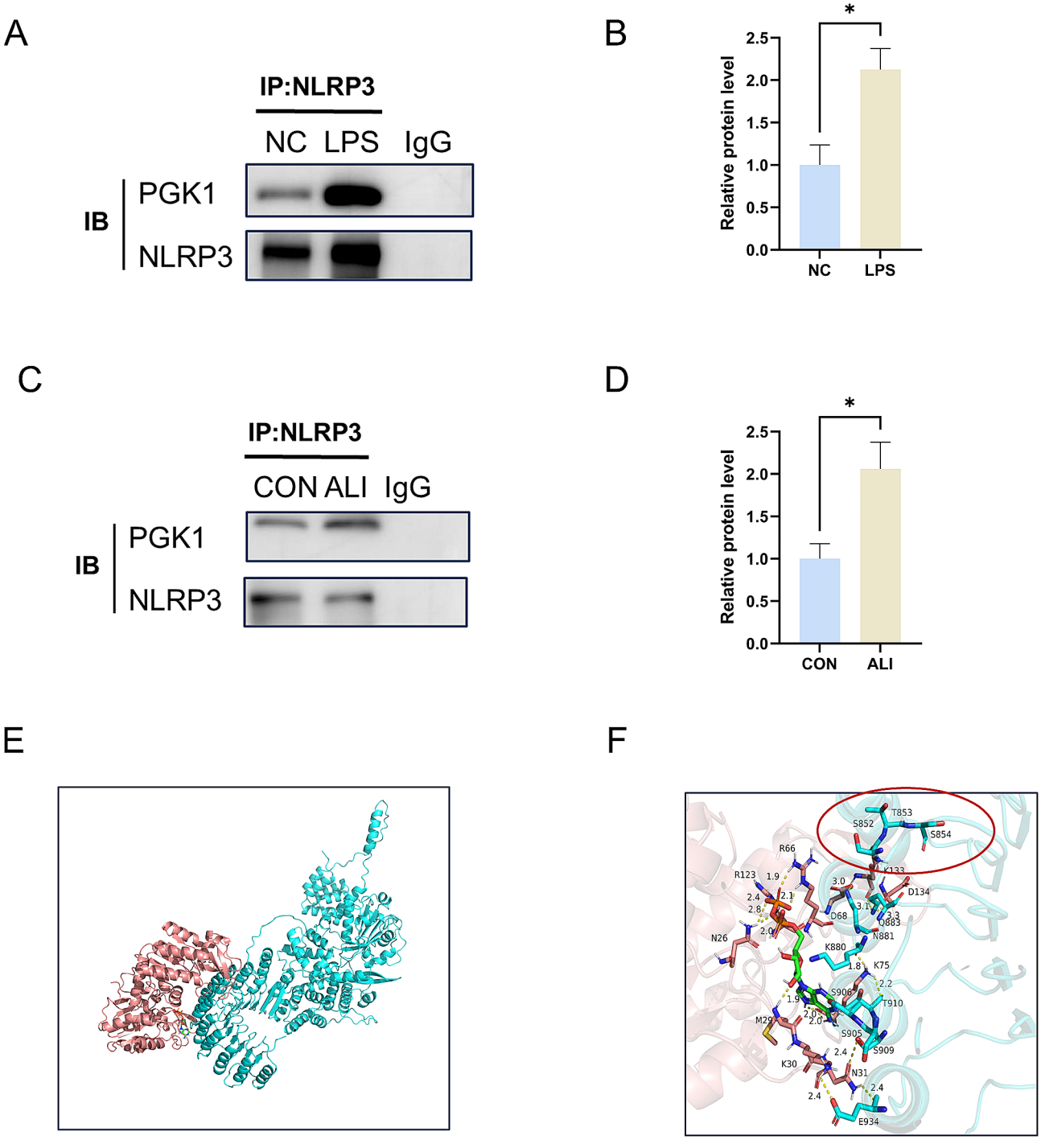

Fig. 5 The association between PGK1 and NLRP3 exhibited an increased affinity after being stimulated by LPS **A**-**B**: Co-IP assays were performed to detect the interaction between NLRP3 and PGK1 using the lysate of BMDMs. **C**-**D**: Co-IP assays were performed to detect the interaction between NLRP3 and PGK1 using the lysate of mice's lung tissue. **E**-**F**: Molecular binding between NLRP3 and PGK1 protein is graphically displayed using the HDOCK Server. The ideal predicted docking position of NLRP3(blue ribbon) on the domain where ADP binds to PGK1(pink ribbon)(**E**). The red circle indicates the specific locations on the amino acid sites where the modification of NLRP3 may occur(**F**). The data shown are the means ± SEM obtained from three separate biological replicates. * $P < 0.05$ by unpaired t test

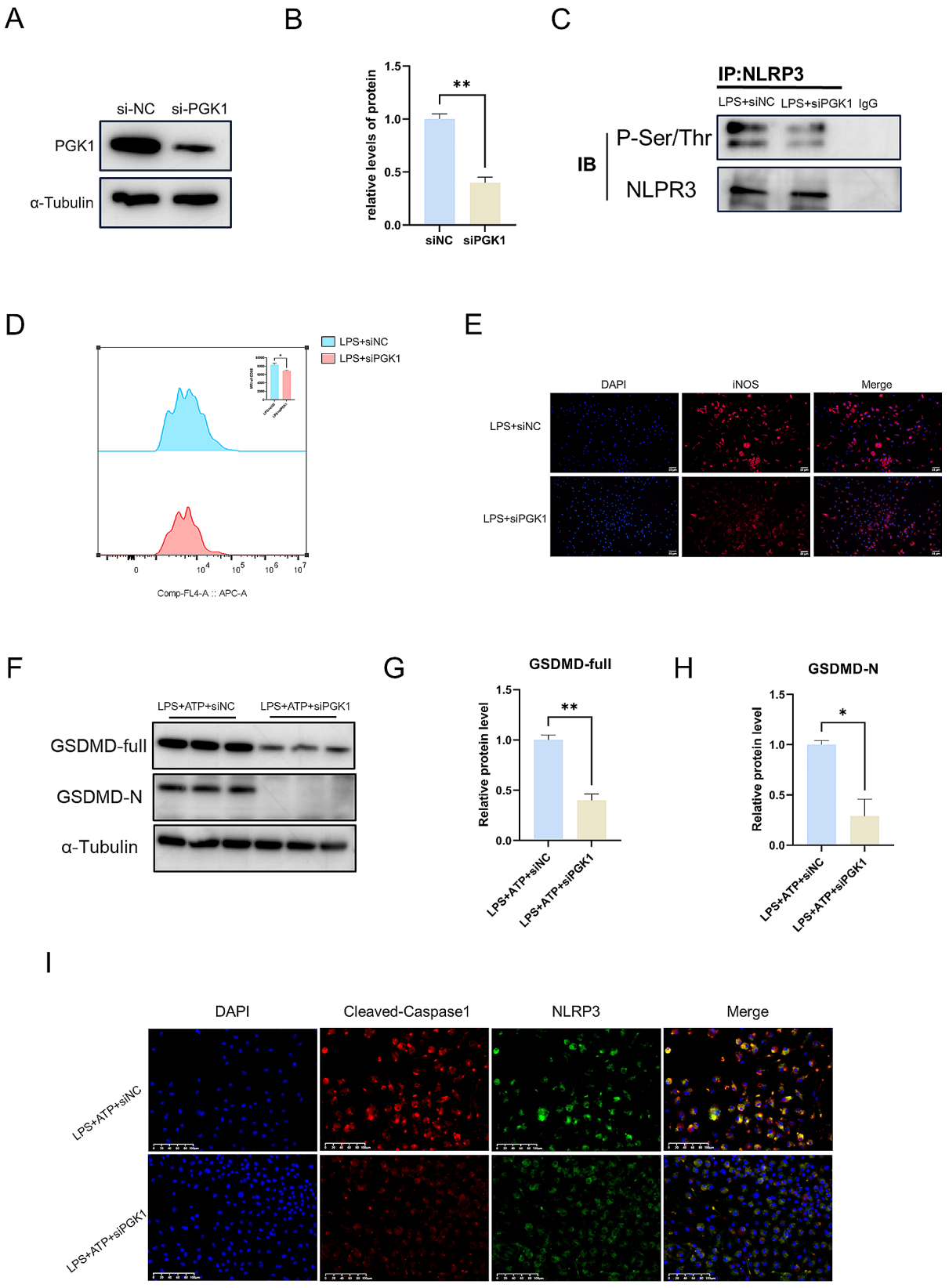

Fig. 6 (See legend on next page.)

(See figure on previous page.)

Fig. 6 Inhibition of PGK1 mitigates M1 macrophages and reduces pyroptosis **A**-**B**: The small interfering RNA (siRNA) was employed to downregulate PGK1 expression in BMDMs. Western blotting analyses the expression of PGK1fig in BMDMs. **C**-**E**: To simulate M1 macrophages, BMDMs were exposed to LPS for a duration of 24 h. Prior to the stimulation, siRNA was administered. Co-IP assays were performed to detect the phosphorylation level of NLRP3 in BMDMs(**C**).CD86 expression on BMDMs was detected by flow cytometry after gating with the macrophage marker F4/80. MFI analysis was conducted to compare the expression of CD86 in BMDMs with the siNC group(**D**). Immunofluorescence analysis of iNOS(Red) staining(scale bar 50 μm) (**E**). **F**-**I**: The cells underwent pre-stimulation with LPS for a duration of 4 h. Afterward, the cells were activated with ATP to induce the pyroptosis model. Protein levels of GSDMD in BMDMs were determined by Western blotting(**F**-**H**). Immunofluorescence staining for the colocalization of NLRP3(Green) and Cleaved-caspase1(Red) (scale bar 100 μm) (**I**). The data shown are the means ± SEM obtained from three separate biological replicates. * $P < 0.05$, ** $P < 0.01$ by unpaired t test

Pharmacologically inhibiting PGK1 reduces the inflammatory response in a mouse model of ALI

Given the outcomes of the in vivo trials detailed above, we were interested about the specific function of PGK1 in the setting of ALI. First, we administered the PGK1 inhibitor NG52 to the mice. In contrast to the ALI group, the NG52 intervention significantly reduced histological lesions in the lung, although this effect was not dose-dependent (Fig. 7A-B). In addition, Western blotting analysis demonstrated that the expression of pyroptosis-related genes, including NLRP3, GSDMD, and IL-1β, was reduced by NG52 in comparison to ALI mice (Fig. 7C-G). In summary, these findings demonstrated that NG52 effectively suppressed the level of inflammation in vivo in cases of ALI.

Discussion

In the present study, we first found that M1 macrophage activation and macrophage pyroptosis in the macrophages of ALI lung tissues and demonstrated that blocking glycolysis with 2-DG significantly reduced the inflammatory reponses either in vivo or in vitro. By using IP-MS, we found that there was a interaction between PGK1 and NLRP3.What's more, both in vivo and in vitro, the interaction between PGK1 and NLPR3 shown a stronger affinity after treatment with LPS. We also discovered that suppressing PGK1 in LPS-stimulated BMDMs reduced the degree of NLRP3 phosphorylation. M1 macrophage activation and macrophage pyroptosis were reduced by the inhibition of PGK1 in vitro. Furthermore, we noticed that NG52 restricted the inflammatory response in mice with ALI.

The alteration of cellular metabolic pathways in order to meet energy demands under varying environmental conditions, thereby enhancing cell resilience against external stress [23]. Recently, Loads of work have demonstrated that metabolic reprogramming plays a pivotal role in macrophage activation [24]. Evanna and colleagues shed light on the critical role of the enhanced production of succinate in regulating macrophage ROS production [25]. Min Kong et al. confirmed that the inhibition of glycolysis activator 6-phosphofructo-2-kinase/fructose-2,6 biphosphatase 3 (PFKFB3) could reduce the pro-inflammatory cytokine secretion in macrophages [11]. However, the exact metabolic alteration that induced in macrophage activation that promotes the disease processes remain largely unknown. It is essential to explore the specific mechanisms linking metabolic reprogramming and inflammation and to develop the novel target to downregulate inflammation in various inflammatory diseases. Here, we established a LPS-induced ALI model treated with glycolysis inhibitor 2-DG. In keeping with previous studies, the results showed that 2-DG exerted an anti-inflammatory effect in the ALI mice. What'more, we found that inhibiting glycolysis by 2-DG reduced both M1 macrophage activation and macrophage pyroptosis.

PGK1 is one of two ATP-generating enzymes in glycolysis, thus has been thought of a key factor in energy homeostasis [26]. Recently, there has been an increasing interest in the role of PGK1 in regulating metabolism and inflammation. Previous research has demonstrated that PGK1 expression can partially reflect glycolysis activity [27, 28]. Cao W's research found that PGK1 plays a crucial role in facilitating microglial M1 polarization and inflammation induced by ischemia/reperfusion injury through the regulation of glycolysis [29]. Furthermore, a recent study regarding myocarditis discovered that the activation of PGK1 may have led to an increased flow of the glycolytic pathway in order to meet the energy and synthesis needs of $CD4^+$ T and Th17 cells [18]. In addition to its role as a glycolytic enzyme, PGK1 also serves as a protein kinase in numerous biological processes [30]. Xie et al. found that PKM2-mediated glycolysis facilitates the inflammasome activation by modifying EIF2AK2 phosphorylation [31]. We wonder if PGK1 controls the production of pro-inflammatory compounds in a similar way to PKM2, given the similarities in their functions. Thus, this implies that PGK1 may modulate inflammation through its regulation of glycolysis or its kinase activity.

To date, there is a paucity of studies elucidating the role of PGK1 in the regulation of inflammation during ALI. In our study, we first found the interaction between PGK1 and NLRP3.We observed that targeting PGK1 by siRNA significantly decreased the macrophage M1 activation and weakened macrophage pyroptosis in BMDMs. In conclusion, our findings expand the current understanding of glycolysis in ALI and also identify a potential novel target for reducing inflammation in the disease.

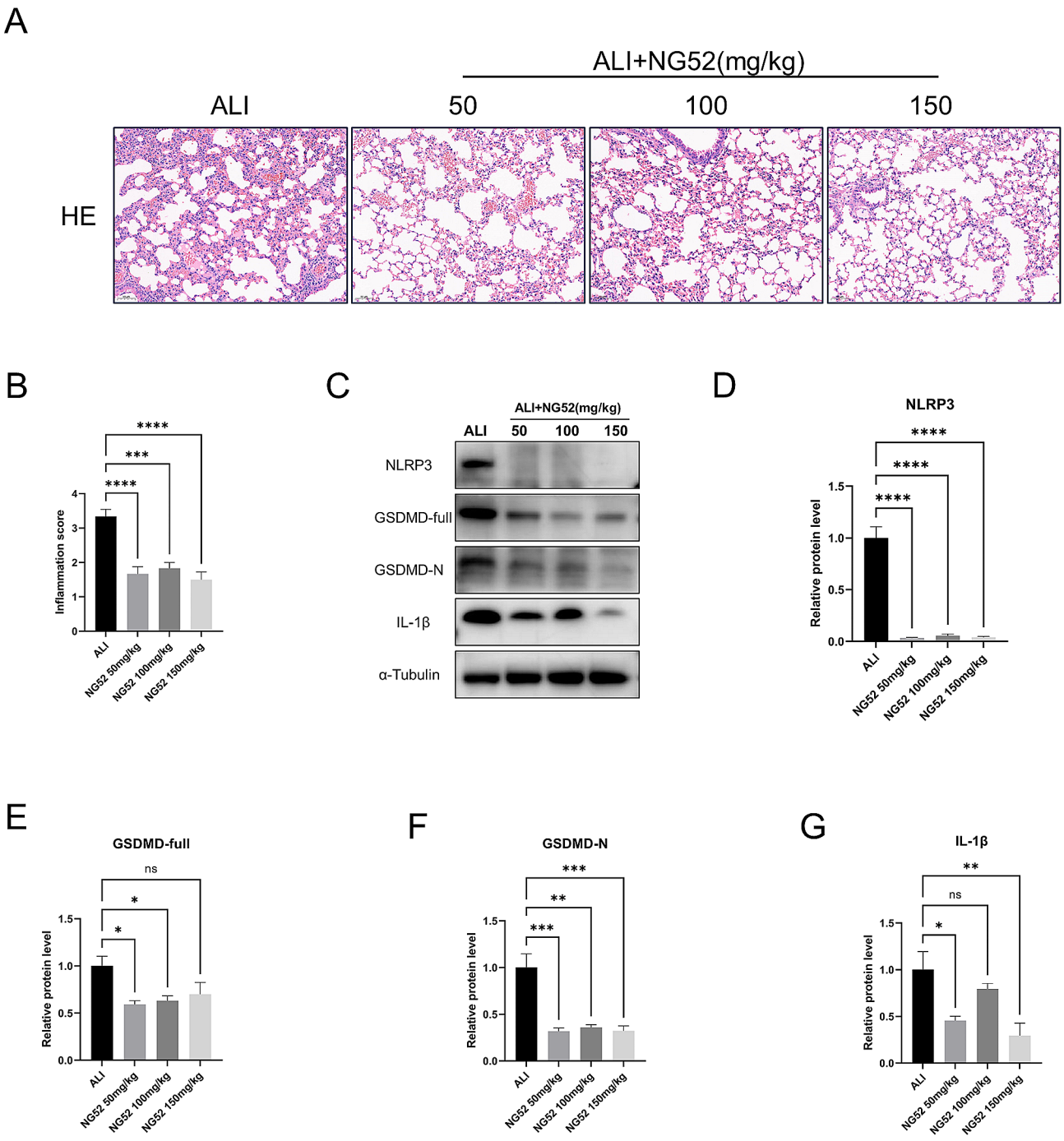

Fig. 7 Pharmacologically inhibiting PGK1 reduces the inflammatory response in a mouse model of ALI C57BL/6J mice were gavaged with NG52 one hour prior to the administration of LPS. **A**-**B**: Evaluation of the therapeutic effect of NG52 on the lung tissue of ALI mice by HE staining (scale bar 50 μm). Inflammation score was measured. **C**-**G**: Western blotting analyses the expression of pyroptosis molecules NLRP3, GSDMD, IL-1β in lung. Immunoblot analysis of pyroptosis molecules NLRP3, GSDMD, IL-1β expression in lung, compared with the ALI group. The data shown are the means ± SEM obtained from three separate biological replicates. * $P < 0.05$, ** $P < 0.01$, *** $P < 0.001$, **** $P < 0.0001$ by one-way ANOVA

Macrophages serve as central regulators of defense against the pathogen in respiratory diseases [32].Macrophages are highly plastic innate immune cells that could change their function under diverse microenvironment. Moreover, macrophages are polarized to M1 pro-inflammatory phenotype with enhanced glycolysis [33, 34].In recent years, researchers have shown an increased interest in macrophage pyroptosis in ALI. Pyroptosis is a form of inflammatory programmed cell death as a consequence of inflammatory caspases. The

NLRP3-Caspase1 signaling pathway plays a vital role in macrophage pyroptosis [35, 36].A recent study showed that Deh reduced mitochondrial damage led to the reduction of NLRP3-mediated pyroptosis in ALI mice [37]. What's more, Wu et al. found the inhibition of NLRP3 inflammasome activation could reduced TMAO-stimulated M1 features [38].They identified NLRP3 inflammasome activation is an important factor of M1 polarization of macrophages and macrophage pyroptosis. Based on the function of glycolysis in regulating inflammasome activation [39], it's essential to explore the exact mechanisms between glycolysis and NLRP3. We observed that the binding of PGK1 and NLRP3 was significantly increased in LPS-treated group either in vivo or in vitro. Meanwhile, the two have an effective structure for coupling one another. The results of protein-protein docking have given us a molecular basis for how PGK1 might work as an enzyme when it interacts with NLRP3. Additionally, our research revealed that inhibiting PGK1 in LPS-stimulated BMDMs resulted in a decline in the level of NLRP3 phosphorylation. These findings indicated that PGK1 may function as a kinase to phosphorylate NLRP3, hence activating the NLRP3 inflammasome.

There are various limitations inherent in our investigation. Firstly, the absence to conduct research on the modulation of M2 polarization hinders the comprehensive evaluation of macrophage function in ALI. Secondly, further confirmation is needed to determine whether PGK1 functions as a glucose enzyme in macrophage inflammatory response. Thirdly, the investigation did not include an examination of the potential impact on enzyme activity when PGK1 serves as a protein kinase, nor did it involve testing the functional alterations using enzym-active mutants. Thus, additional research is necessary in order to elucidate the precise role of PGK1 in the regulation of NLRP3.

Taken together, our research demonstrates the significant involvement of PGK1 in regulating macrophage inflammatory response through the regulation of NLRP3. The potential use of the PGK1-NLRP3 interaction in macrophages is a promising approach for addressing inflammatory diseases.

Acknowledgements
None.

Author contributions
Guiyin Zhu, Haiyang Yu, and Wen Gu conceived and designed research; Guiyin Zhu, Haiyang Yu, and Tian Peng performed experiments; Guiyin Zhu, Tian Peng, Kun Yang and Xue Xu analyzed and interpreted the data; Guiyin Zhu prepared figures; Guiyin Zhu and Haiyang Yu wrote the manuscript; Guiyin Zhu and Wen Gu revised manuscript; All the authors read and approved the final manuscript.

Funding
This study was supported by the National Natural Science Foundation of China (Grant No. 81770023) and the Science and Technology Innovation Plan of Shanghai Science and Technology Commission (Grant No. 22Y11901700).

Data availability
No datasets were generated or analysed during the current study.

Declarations

Ethics approval and consent to participate
All animal experiments were conducted in accordance with the approved protocols by the Ethics Committee of Xinhua Hospital, affiliated with the Shanghai Jiao Tong University School of Medicine (Approval No, XHEC-F-2023-067).

Consent for publication
Not applicable.

Competing interests
The authors declare no competing interests.

Received: 26 February 2024 / Accepted: 25 July 2024
Published online: 30 July 2024

References

1. Bellani G, Laffey JG, Pham T, Fan E, Brochard L, Esteban A, et al. Epidemiology, patterns of care, and mortality for patients with acute respiratory distress syndrome in intensive care units in 50 countries. JAMA. 2016;315:788–800.
2. Hu Q, Zhang S, Yang Y, Yao J-Q, Tang W-F, Lyon CJ, et al. Extracellular vesicles in the pathogenesis and treatment of acute lung injury. Mil Med Res. 2022;9:1–21.
3. Rubins JB. Alveolar macrophages: wielding the double-edged sword of inflammation. Am J Respir Crit Care Med. American Thoracic Society; 2003. pp. 103–4.
4. Wang K, Rong G, Gao Y, Wang M, Sun J, Sun H, et al. Fluorous-tagged peptide nanoparticles ameliorate Acute Lung Injury via Lysosomal Stabilization and Inflammation Inhibition in Pulmonary macrophages. Small. 2022;18:2203432.
5. Wang L, Zhang H, Sun L, Gao W, Xiong Y, Ma A, et al. Manipulation of macrophage polarization by peptide-coated gold nanoparticles and its protective effects on acute lung injury. J Nanobiotechnol. 2020;18:1–16.
6. Hsu CG, Chávez CL, Zhang C, Sowden M, Yan C, Berk BC. The lipid peroxidation product 4-hydroxynonenal inhibits NLRP3 inflammasome activation and macrophage pyroptosis. Cell Death Differ. 2022;29:1790–803.
7. Zhang K, Shi Z, Zhang M, Dong X, Zheng L, Li G, et al. Silencing lncRNA Lfar1 alleviates the classical activation and pyoptosis of macrophage in hepatic fibrosis. Cell Death Dis. 2020;11:132.
8. Shu B, Zhou Y-X, Li H, Zhang R-Z, He C, Yang X. The METTL3/MALAT1/PTBP1/USP8/TAK1 axis promotes pyroptosis and M1 polarization of macrophages and contributes to liver fibrosis. Cell Death Discov. 2021;7:368.
9. Pålsson-McDermott EM, O'Neill LAJ. Targeting immunometabolism as an anti-inflammatory strategy. Cell Res. 2020;30:300–14.
10. Zhong W-J, Liu T, Yang H-H, Duan J-X, Yang J-T, Guan X-X, et al. TREM-1 governs NLRP3 inflammasome activation of macrophages by firing up glycolysis in acute lung injury. Int J Biol Sci. 2023;19:242.
11. Kong M, Zhu D, Dong J, Kong L, Luo J. Iso-seco-tanapartholide from Artemisia argyi inhibits the PFKFB3-mediated glycolytic pathway to attenuate airway inflammation in lipopolysaccharide-induced acute lung injury mice. J Ethnopharmacol. 2023;301:115781.
12. Zhong W, Yang H, Guan X, Xiong J, Sun C, Zhang C, et al. Inhibition of glycolysis alleviates lipopolysaccharide-induced acute lung injury in a mouse model. J Cell Physiol. 2019;234:4641–54.
13. Bernstein BE, Hol WGJ. Crystal structures of substrates and products bound to the phosphoglycerate kinase active site reveal the catalytic mechanism. Biochemistry. 1998;37:4429–36.
14. Fu Q, Yu Z. Phosphoglycerate kinase 1 (PGK1) in cancer: a promising target for diagnosis and therapy. Life Sci. 2020;256:117863.
15. Li X, Jiang Y, Meisenhelder J, Yang W, Hawke DH, Zheng Y, et al. Mitochondria-translocated PGK1 functions as a protein kinase to coordinate glycolysis and the TCA cycle in tumorigenesis. Mol Cell. 2016;61:705–19.
16. Liao L, Dang W, Lin T, Yu J, Liu T, Li W, et al. A potent PGK1 antagonist reveals PGK1 regulates the production of IL-1β and IL-6. Acta Pharm Sin B. 2022;12:4180–92.

17. Wang Wliang, Jiang Z, ru, Hu C, Chen C, Hu Z, quan, Wang A, li et al. Pharmacologically inhibiting phosphoglycerate kinase 1 for glioma with NG52. Acta Pharmacol Sin [Internet]. 2021 [cited 2024 Jun 7];42:633–40. https://pubmed.ncbi.nlm.nih.gov/32737469/
18. Lu Y, Zhao N, Wu Y, Yang S, Wu Q, Dong Q et al. Inhibition of phosphoglycerate kinase 1 attenuates autoimmune myocarditis by reprogramming CD4 + T cell metabolism. Cardiovasc Res [Internet]. 2023 [cited 2024 Jun 6];119:1377–89. https://pubmed.ncbi.nlm.nih.gov/36726197/
19. Li D, Yang L, Wang W, Song C, Xiong R, Pan S et al. Eriocitrin attenuates sepsis-induced acute lung injury in mice by regulating MKP1/MAPK pathway mediated-glycolysis. Int Immunopharmacol [Internet]. 2023 [cited 2024 Jun 7];118. https://pubmed.ncbi.nlm.nih.gov/36966548/
20. Zhang J, Liu X, Wan C, Liu Y, Wang Y, Meng C, et al. NLRP3 inflammasome mediates M1 macrophage polarization and IL-1β production in inflammatory root resorption. J Clin Periodontol. 2020;47:451–60.
21. Anand PK. Lipids, inflammasomes, metabolism, and disease. Immunol Rev. 2020;297:108–22.
22. Lu Z, Hunter T. Metabolic kinases moonlighting as protein kinases. Trends Biochem Sci. 2018;43:301–10.
23. Gaber T, Strehl C, Buttgereit F. Metabolic regulation of inflammation. Nat Rev Rheumatol. 2017;13:267–79.
24. n den Bossche J, O'Neill LA, Menon D. Macrophage immunometabolism: where are we (going)? Trends Immunol. 2017;38:395–406.
25. Mills EL, Kelly B, Logan A, Costa ASH, Varma M, Bryant CE, et al. Succinate dehydrogenase supports metabolic repurposing of mitochondria to drive inflammatory macrophages. Cell. 2016;167:457–70.
26. Zhang Y, Yu G, Chu H, Wang X, Xiong L, Cai G, et al. Macrophage-associated PGK1 phosphorylation promotes aerobic glycolysis and tumorigenesis. Mol Cell. 2018;71:201–15.
27. Li W, Xu M, Li Y, Huang Z, Zhou J, Zhao Q et al. Comprehensive analysis of the association between tumor glycolysis and immune/inflammation function in breast cancer. J Transl Med [Internet]. 2020 [cited 2024 Jun 8];18. https://pubmed.ncbi.nlm.nih.gov/32070368/
28. Cai R, Zhang Y, Simmering JE, Schultz JL, Li Y, Fernandez-Carasa I, et al. Enhancing glycolysis attenuates Parkinson's disease progression in models and clinical databases. J Clin Invest. 2019;129:4539–49.
29. Cao W, Feng Z, Zhu D, Li S, Du M, Ye S et al. The Role of PGK1 in Promoting Ischemia/Reperfusion Injury-Induced Microglial M1 Polarization and Inflammation by Regulating Glycolysis. Neuromolecular Med [Internet]. 2023 [cited 2024 Jun 8];25:301–11. https://pubmed.ncbi.nlm.nih.gov/36749430/
30. Liu H, Wang X, Shen P, Ni Y, Han X. The basic functions of phosphoglycerate kinase 1 and its roles in cancer and other diseases. Eur J Pharmacol. 2022;920:174835.
31. Xie M, Yu Y, Kang R, Zhu S, Yang L, Zeng L, et al. PKM2-dependent glycolysis promotes NLRP3 and AIM2 inflammasome activation. Nat Commun. 2016;7:13280.
32. Malainou C, Abdin SM, Lachmann N, Matt U, Herold S. Alveolar macrophages in tissue homeostasis, inflammation, and infection: evolving concepts of therapeutic targeting. J Clin Invest. 2023;133.
33. Helou DG, Quach C, Hurrell BP, Li X, Li M, Akbari A et al. LAIR-1 limits macrophage activation in acute inflammatory lung injury. Mucosal Immunol. 2023.
34. Meng Y, Kong K, Chang Y, Deng X, Yang T. Histone methyltransferase SETD2 inhibits M1 macrophage polarization and glycolysis by suppressing HIF-1α in sepsis-induced acute lung injury. Med Microbiol Immunol. 2023;1–11.
35. Man SM, Karki R, Kanneganti T. Molecular mechanisms and functions of pyroptosis, inflammatory caspases and inflammasomes in infectious diseases. Immunol Rev. 2017;277:61–75.
36. Mishra PK, Adameova A, Hill JA, Baines CP, Kang PM, Downey JM et al. Guidelines for evaluating myocardial cell death. Am J Physiol Heart Circ Physiol. 2019.
37. Pu Z, Sui B, Wang X, Wang W, Li L, Xie H. The effects and mechanisms of the anti-COVID-19 traditional Chinese medicine, Dehydroandrographolide from Andrographis paniculata (burm. f.) wall, on acute lung injury by the inhibition of NLRP3-mediated pyroptosis. Phytomedicine. 2023;114:154753.
38. Wu K, Yuan Y, Yu H, Dai X, Wang S, Sun Z, et al. The gut microbial metabolite trimethylamine N-oxide aggravates GVHD by inducing M1 macrophage polarization in mice. Blood J Am Soc Hematol. 2020;136:501–15.
39. Próchnicki T, Latz E. Inflammasomes on the crossroads of innate immune recognition and metabolic control. Cell Metab. 2017;26:71–93.

Publisher's Note